Meteorol. Atmos. Phys. 78, 115–132 (2001)

Meteorology and Atmospheric Physics

[1] Institute of Meteorology, University of Bonn, Germany
[2] Polar Meteorology Group, Byrd Polar Research Center, The Ohio State University
[3] Atmospheric Science Program, Department of Geography, The Ohio State University

Mesoscale modeling of katabatic winds over Greenland and comparisons with AWS and aircraft data

T. Klein[1], **G. Heinemann**[1], **D. H. Bromwich**[2,3], **J. J. Cassano**[2], and **K. M. Hines**[2]

With 11 Figures

Received September 22, 2000
Revised March 16, 2001

Summary

Simulations of the katabatic wind system over the Greenland ice sheet for the two months April and May 1997 were performed using the Norwegian Limited Area Model (NORLAM) with a horizontal resolution of 25 km. The model results are intercompared and validated against observational data from automatic weather stations (AWS), global atmospheric analyses and instrumented aircraft observations of individual cases during that period. The NORLAM is able to simulate the synoptic developments and daily cycle of the katabatic wind system realistically. For most of the cases covered by aircraft observations, the model results agree very well with the measured developments and structures of the katabatic wind system in the lowest 400 m. Despite NORLAM's general ability of reproducing the four-dimensional structure of the katabatic wind, problems occur in cases, when the synoptic background is not well captured by the analyses used as initial and boundary conditions for the model runs or where NORLAM fails to correctly predict the synoptic development. The katabatic wind intensity in the stable boundary layer is underestimated by the model in cases when the simulated synoptic forcing is too weak. An additional problem becomes obvious in cases when the model simulates clouds in contrast to the observations or when the simulated clouds are too thick compared to the observed cloud cover. In these cases, the excessive cloud amount prevents development of the katabatic wind in the model.

1. Introduction

Katabatic winds are common phenomena over the sloped ice sheets of Greenland and Antarctica. They are gravity-driven downslope flows which form as a result of the cooling of the near surface air over the sloped ice sheet due to the divergence of radiation and sensible heat fluxes. Most intense katabatic winds with wind speeds up to gale force are found in the coastal zones, where a strong topographic gradient is present (Putnins, 1970; Ball, 1956; Wendler, 1990). The so-called "piteraq", which is a strong synoptically enforced katabatic wind at the Greenlandic coast, represents a well-known phenomenon to the Inuits at Greenland (Rasmussen, 1989). Because of the large scale of the katabatic wind regime, the Coriolis force is important, resulting in a deviation from the downslope direction to the right on the Northern Hemisphere.

Most investigations of the Greenland katabatic wind system rely on surface observations and numerical simulations. However, detailed analyses of the three-dimensional structure of katabatic winds and their evolution in time are rare because of the lack of suitable validation data sets. The situation changed with the Greenland Ice Margin Experiment (GIMEX) in 1991 (Oerlemans and Vugts, 1993) in combination with the ETH Greenland Expedition, which included turbulence measurements up to 30 m over the ice (Forrer and Rotach, 1997), and also remote sensing measurements of the boundary layer over the ice (Meesters et al., 1997). A further significant improvement was achieved with the performance of the experiment KABEG 97 (Katabatic Wind and Boundary Layer Front Experiment around Greenland, hereafter KABEG) in the area of Kangerlussuaq (also known as Søndre Strømfjord, 67°01′32″ N, 50°36′11″ W, Western Greenland) during April and May 1997 (Heinemann, 1998, 1999). During KABEG, five surface stations were installed at different locations on the ice sheet and in the tundra area near Kangerlussuaq (see Figs. 1 and 2). In addition to these surface measurements, nine individual cases of katabatic wind developments were investigated by aircraft measurements. These katabatic wind flights were performed under very different synoptic conditions and thereby allow for the study of the impact of the synoptic environment on the development of katabatic winds. Furthermore, the surface conditions during the flights were different, since during the KABEG period melting occured in the tundra area, which was almost snow-free at the end of KABEG.

After successful early simulations of katabatic winds in Antarctica using the simple steady-state model of Ball (1956, 1960) like in Parish and Bromwich (1987), further advances were achieved by the application of three-dimensional mesoscale models using the primitive equations for the numerical simulation of these wind systems. While Heinemann (1997), Gallée (1995), and Bromwich et al. (1994) use idealized initial and boundary conditions for the simulation of Antarctic katabatic winds in the Weddell Sea Region and the Ross Sea Area, respectively, Hines et al. (1995) perform a simulation for the period of June 1988 using a mesoscale model nested into global analyses for Antarctica. For Greenland, Heinemann (1996) and Bromwich et al. (1996) show characteristic features of Greenland katabatic winds, again applying idealized initial and boundary conditions.

In the present paper, the three-dimensional structure of the katabatic wind system over Greenland and its evolution in time is investigated by numerical simulations with the Norwegian limited area model (NORLAM), which is nested into analyses provided by the European Centre for Medium-range Weather Forecasts (ECMWF). The simulations cover all cases of the KABEG katabatic wind flights. Comparisons of the NORLAM results to the aircraft measurements are performed. Additionally, the available data of the KABEG AWS and observations from the Program for Arctic Regional Climate Assessment (PARCA) Greenland Climate Network (GC-Net) AWS (Steffen et al., 1996) were used for the validation of NORLAM.

The outline of the present paper is as follows: A description of the NORLAM is given in Sect. 2. In Sect. 3, the results of the NORLAM runs are presented with an emphasis on the comparisons to the AWS and aircraft data, and Sect. 4 contains a summary.

2. The numerical model and data description

2.1 NORLAM

The Limited Area Model (LAM) used for the simulations is the former operational DNMI (The Norwegian Institute, Oslo) model NORLAM (version 9). A general description of the model and its parameterizations is given in Grønås and Hellevik (1982), and in Nordeng (1986), while a summary of the characteristics of the version 9 NORLAM can be found in Table 1.

For the studies of the present paper, a nesting mode is used. A first run with a 50 km grid

Table 1. Characteristics of NORLAM (version 9)

NORLAM	
grid	modified Arakawa D (Grønås and Hellevik, 1982)
vertical coordinate	σ-type
vertical levels	30/40 σ-levels
equations of motion	primitive, hydrostatic
initialization	iterative normal mode (Bratseth, 1982)
boundary layer	Louis (1979), Blackadar (1979)
surface layer, radiation	Nordeng (1986)
convection scheme	modified Kuo (1965) scheme
surface categories	water, sea ice, ice, land, ablation zone, tundra

(LAM50) is performed using ECMWF analyses as initial conditions. A second integration with a 25 km grid (LAM25) is then executed starting with the 0 h initialized analyses of the LAM50 run as initial conditions. ECMWF analyses were taken as boundary fields for the LAM50 runs, while for the 25 km simulation the results of the LAM50 run were used as boundary values. The model is used with a domain size of 121×97 grid points for the LAM50 and LAM25 simulations. The validation study compares observations with results of only the LAM25. LAM50 results are used for a comparison with ECMWF data in order to check NORLAM's ability of reproducing the large-scale atmospheric conditions. The months April and May 1997 were completely simulated with a vertical resolution of 30 σ-levels. The model was operated in a forecast mode, i.e. it was restarted with a new ECMWF analysis at 0000 UTC every day and integrated forward in time for 48 hours. Therefore, each day of the month apart from the first day is covered by integrations twice.

For the simulation of the katabatic wind system during the individual KABEG cases, model reruns with three different start times of NORLAM were performed, i.e. each flight case was simulated three times using different ECMWF analyses as initial fields. The first simulation starts one day prior to the flight at 0000 UTC, the second on the day before the flight at 1200 UTC, and the third simulation starts on the day of the flight at 0000 UTC (aircraft missions started at about 0700 UTC). In order to provide a high vertical resolution for the comparison of the model results to the aircraft-obtained boundary layer profiles of KABEG (see below), the vertical resolution of NORLAM was increased to 40 σ-levels for the reruns. A very good resolution of the boundary layer is achieved, since 18 of the 40 σ-levels are located in the lowest 400 m of the atmosphere with 5 levels covering the lowest 100 m.

The model domain of the NORLAM grid LAM50 which is used for all the simulations presented in this paper is displayed in Fig. 1a. The LAM50 domain ranges from Canada to Europe while the domain of the inner grid LAM25 (Fig. 1b, indicated by the rectangle in Fig. 1a) only captures Greenland. The region of Kangerlussuaq, where six of the KABEG flights took place and where the KABEG AWS were operated, is marked by a box in Fig. 1b and shown in detail in Fig. 1c.

The input data used for the simulations is listed in Table 2. In order to account for the complex topography of the tundra, which cannot be explicitly resolved with the grid spacings used, a larger roughness $z_0 = 10^{-2}$ m was introduced for grid points within the tundra area. The tundra grid points were identified using the variance of a sub-grid scale topography with 2.2 km resolution (Ekholm, 1996). The tundra area is ice-covered during most of the year apart from the summer months May to August. For the simulation of May 1997, the tundra area in the model is therefore ice-free. This is in agreement with the satellite (AVHRR visible channels) and in-situ observations during KABEG, which showed a sudden melting of the tundra snow at the end of April (Heinemann, 1998, 1999). The surface class "tundra" was not used for the monthly simulations of April 1997, and the tundra was treated as inland ice ($z_0 = 10^{-4}$ m). The simulation for the month May 1997, however, as well as the individual reruns with increased vertical resolution for the KABEG flights were performed with the additional "tundra" surface class. A larger roughness of the ice surface can be found in the so-called ablation zones close to the coast of Greenland, where the strongest topographical gradients are present. The processes of melting, runoff and ice dynamics lead to a significant modification of the surface characteristics in the ablation zone and were therefore taken into account using an additional surface class for the simulations. For the surface class "ablation zone" (contained in all discussed simulations), a z_0 value of 10^{-2} m was chosen, and the gradient of the gridscale topography (exceeding 1%) was used to identify the grid points within the ablation zone.

The months April and May 1997 were simulated twice using different albedos of 0.6 and 0.8 for the ice sheet, respectively. Since comparisons with the available AWS data and aircraft-measured albedo during KABEG suggested that an albedo of 0.8 for the ice sheet was more realistic, only the simulation results of the runs with an albedo of 0.8 are discussed in the present paper.

2.2 Observational data

Observational data collected during the aircraft-based experiment KABEG during April/May 1997

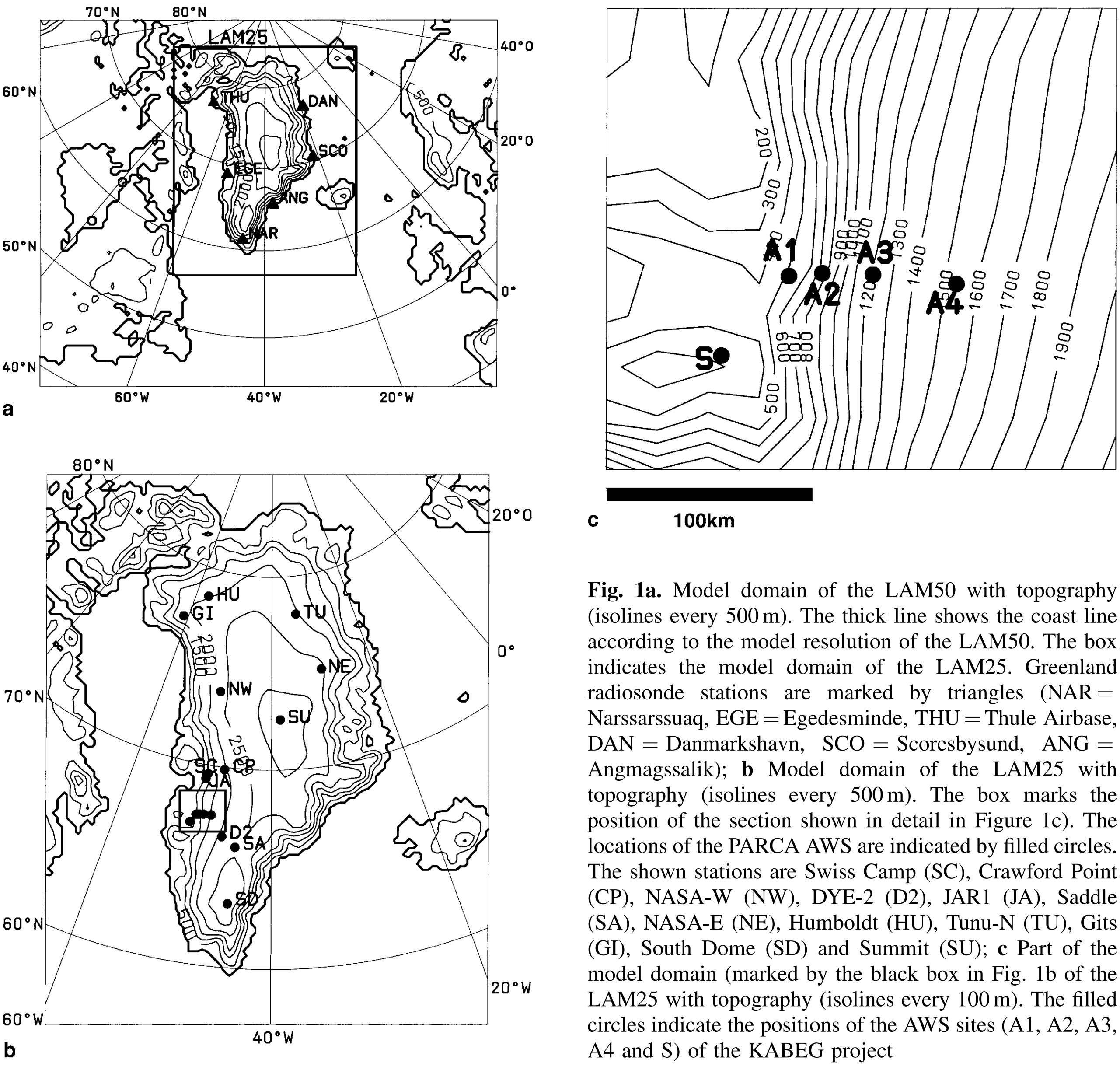

Fig. 1a. Model domain of the LAM50 with topography (isolines every 500 m). The thick line shows the coast line according to the model resolution of the LAM50. The box indicates the model domain of the LAM25. Greenland radiosonde stations are marked by triangles (NAR = Narssarssuaq, EGE = Egedesminde, THU = Thule Airbase, DAN = Danmarkshavn, SCO = Scoresbysund, ANG = Angmagssalik); **b** Model domain of the LAM25 with topography (isolines every 500 m). The box marks the position of the section shown in detail in Figure 1c). The locations of the PARCA AWS are indicated by filled circles. The shown stations are Swiss Camp (SC), Crawford Point (CP), NASA-W (NW), DYE-2 (D2), JAR1 (JA), Saddle (SA), NASA-E (NE), Humboldt (HU), Tunu-N (TU), Gits (GI), South Dome (SD) and Summit (SU); **c** Part of the model domain (marked by the black box in Fig. 1b of the LAM25 with topography (isolines every 100 m). The filled circles indicate the positions of the AWS sites (A1, A2, A3, A4 and S) of the KABEG project

in the area of South Greenland constitute the main data set for the validation of the numerical model. The goals of the katabatic wind program of KABEG were to investigate the development of the katabatic flow under high pressure conditions, the channeling of the katabatic flow and effects of synoptic forcing, and the modification of the katabatic flow in the transition zones ice/ocean and ice/tundra. During the planning of the katabatic wind flights of KABEG, model simulations were also taken into account. The area near Kangerlussuaq (K1, Fig. 2) was selected to investigate the development of the katabatic flow over relatively homogeneous topography and the modification of the katabatic flow in the transition zone ice/tundra. The regions for the investigation of channeling effects of the katabatic wind were near Ilulissat (K3) and southwest of Tasiilaq (Angmagssalik)/ Kulusuk (K2), where pronounced valley structures with steep topographic gradients are present.

In the K1 area, automatic surface stations were installed along a line oriented parallel to the fall

Table 2. List of data sets and initial settings used for the NORLAM simulations

Input data		
initial and boundary data	ECMWF Tropical Ocean – Global Atmosphere (TOGA), 2.5 °C, 12-hourly analyses	
topography	NOAA (1995), TBASE 8 km resolution	
sea ice coverage	SSM/I-derived (April and May 1997), [algorithm of Cavalieri et al. (1995)]	
sea surface temperature (SST)	Reynolds and Smith (1994), monthly mean, 1 °C resolution	
tundra surfaces	identified by variance of sub-grid scale topography (Ekholm, 1996)	
Surface types	**Albedo**	**Roughness (z_0) in m**
open water	0.15	Charnock relation (minimum 1.5E-5)
sea ice	0.6	1.E-2
ice sheet	0.6/0.8	1.E-4
land (without snow cover)	0.25	3.E-1
ablation zone	0.6/0.8	1.E-2
tundra (not April 1997)	0.25 (ice-free) – 0.5/0.7	1.E-2

line at about 50 km north of Kangerlussuaq (Fig. 2): A1 over the tundra close to the edge of the inland ice (at a distance of 12 km to the ice edge); A2 over the inland ice close to the ice edge (both being wind recorders); and two surface energy balance stations over the ice at distances of about 30 km (A3) and 75 km (A4) from the ice edge.

Aircraft data were collected by the research aircraft POLAR2 (Dornier 228) owned by the Alfred-Wegener-Institut (Bremerhaven, Germany). The GPS-navigated aircraft measured position, wind vector, air temperature and humidity with several instruments with sampling rates between 12 and 120 Hz (Table 3). In addition, downward and upward solar and terrestrial radiation and surface temperature were measured; a high-resolution laser altimeter registered surface roughness structures. Only wind and temperature data are used for the comparison with model results. The aircraft sensors represent a high-quality measurement system, and the errors of the temperature and horizontal wind components can be estimated to be about 0.2 °C and 0.3 ms^{-1}, respectively.

The aircraft data used in this study are vertical profiles flown as slantwise aircraft temps (ascents or descents). Since the aircraft temps were generally performed with a descent/ascent rate corresponding to 5 ms^{-1} relative to the surface, the horizontal distance of two consecutive temps is about 5 km. Details about the KABEG experiment and the instrumentation of the aircraft and surface stations are given in Heinemann (1999).

The locations of the AWS of the PARCA project are shown in Fig. 1b. As shown in Fig. 2, PARCA stations Swiss Camp and JAR1 lie inside the KABEG K3 area. For the validation of NORLAM, five PARCA stations with nearly complete data records for the months April and May 1997 were chosen in order to represent different regions of Greenland. In addition, the comparison of the NORLAM results to one of the KABEG stations will be described in more detail in Sect. 3.2, while the comparisons for the other stations, which yielded similar results, are not discussed in the present paper.

3. Results of the simulations

In this section, the results of the NORLAM simulations for April and May 1997 and for individual katabatic wind cases of the KABEG project are described. The model results are validated using the ECMWF analyses, the data of the surface observations (PARCA AWS and KABEG AWS) and the available aircraft data of KABEG.

3.1 Comparisons of the NORLAM forecasts to the ECMWF analyses

The months April and May 1997 were completely simulated by NORLAM in a forecast mode. For

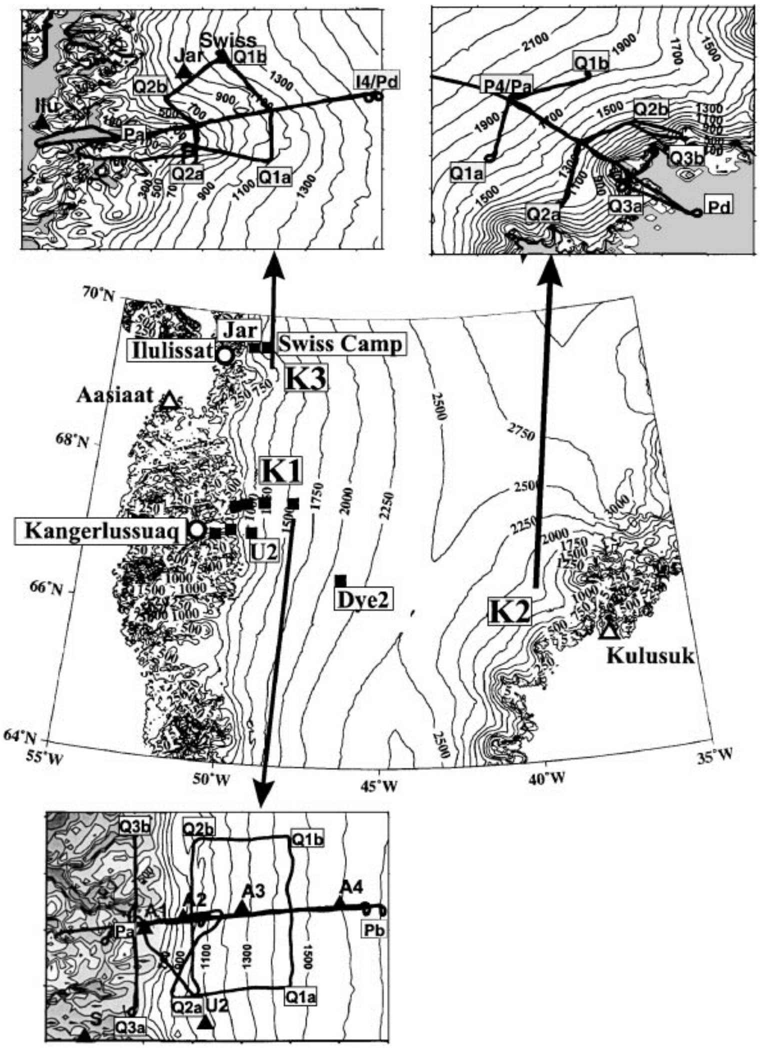

Fig. 2. Locations of the KABEG flight patterns for the three flight areas Kangerlussuaq (K1), Angmagssalik (K2) and Ilulissat (K3). The locations that were chosen for profile comparisons are marked by the triangle A4 in the K1 area, the label P4/Pa in the K2 area and the label I4/Pd in the K3 area

each day of the month, a 48 h simulation was carried out. Monthly mean fields were calculated from the NORLAM results using only the output of the second day of the forecasts. These monthly mean fields were compared to monthly mean fields of the ECMWF analyses, which had been taken as initial and boundary fields for the NORLAM integrations. The large-scale mean structures are well captured by the NORLAM forecasts (not shown), which reflects that the average synoptic conditions are generally well reproduced by NORLAM. The bias (mean NORLAM–mean ECMWF) of the horizontally averaged (over the whole model domain) geopotential height on pressure surfaces is less than 10 m throughout the troposphere during April and May 1997. No excessive moisture loss or production by NORLAM is present, and biases in zonal and meridional wind speed are less than $0.5\,\mathrm{ms}^{-1}$.

In addition, individual comparisons of the synoptic-scale features for the case studies of the KABEG katabatic wind flights underline that the basic large-scale conditions are relatively well captured by NORLAM.

3.2 Validation of the NORLAM against AWS data

3.2.1 Monthly time series and statistics

The NORLAM simulations for the months April and May 1997 were validated against the available AWS data of the PARCA and the KABEG stations. While for the model the surface pressure at the respective height of the grid point, the 2 m

Table 3. Instrumentation of the research aircraft POLAR2 during KABEG

Quantity	Sampling in Hz	Measurement system, instrument
		METEOPOD
Air temperature	120	PT100 open wire (Rosemount)
Air temperature	120	PT100 open wire (AWI)
Air humidity	120	Lyman-α (AIR)
Air humidity	12	Humicap, PT100 in Rosemount housing (Aerodata)
Air humidity	12	Dew point mirror (Gen. Eastern)
Air pressure	12	Pressure sensor (Rosemount)
3D wind vector	120	5-hole-probe (Rosemount)
Acceleration	60	Attitude and Heading Reference System LTR81 (Litton)
Height	120	Radar altimeter (TRT)
		Basic instrumentation
Acceleration	60	LaserNav Inertial Platform Navigation (Honeywell)
Height	12	Radar altimeter
Position	12	GPS (SEL)
Surface temperature	12	KT4 (Heimann), 8–14 µm, 0.6° opening angle
Downward and upward radiation fluxes	12 12	Short-wave: pyranometer (Eppley PSP) Long-wave: pyrgeometer (Eppley PIR)
		Additional instrumentation
Height	500	Laser altimeter (Ibeo)

temperature and the 10 m wind were used, AWS values were taken at the specific sensor heights (between about 2 m and 4 m, also depending on the snow heights at the locations). No height corrections for the difference between the surface elevation on the model grid and the reported elevations of the AWS were made.

In Fig. 3 measured and simulated time series of surface pressure, near surface temperature, wind speed and wind direction are displayed for the PARCA AWS Humboldt (HU in Fig. 1b) for the period of April and May 1997. Humboldt was chosen in order to represent the northwestern part of Greenland. The course of the surface pressure is captured well by NORLAM, and the time series of the NORLAM 2 m temperature shows a good agreement with the measured temperatures at Humboldt. Large-scale changes and the daily courses are captured well by the model. The simulated wind speeds at 10 m height agree reasonably well with the measurements. Considering the difference between sensor (2–4 m) and model height (10 m) above ground, a first guess of a 10 m value from the AWS data can be achieved by adding 10% to the measured values (according to a logarithmic wind profile with $z_0 = 10^{-4}$ m). This height difference can at least partly explain the larger NORLAM wind speeds. A general difficulty for the model simulations seems to be the higher variability of the wind on relatively short time scales compared to temperature and pressure, which vary more slowly and by smaller amplitudes than the winds. As a consequence, the agreement between modeled and measured wind speeds is less satisfactory than the agreement in pressure and temperature. Considering the wind direction, the agreement of model and AWS is very good although daily variations are not as well captured as variations on longer time scales.

From the five KABEG stations, the AWS A4 was chosen for the comparisons, since it has the highest location over the ice (i.e., being farthest from the ice edge and over relatively homogeneous terrain) and should be captured well by the model. The other KABEG AWS, especially S and A1 are located in the complex tundra area, whose small-scale topographic structures cannot be explicitly resolved by a numerical model with 25 km

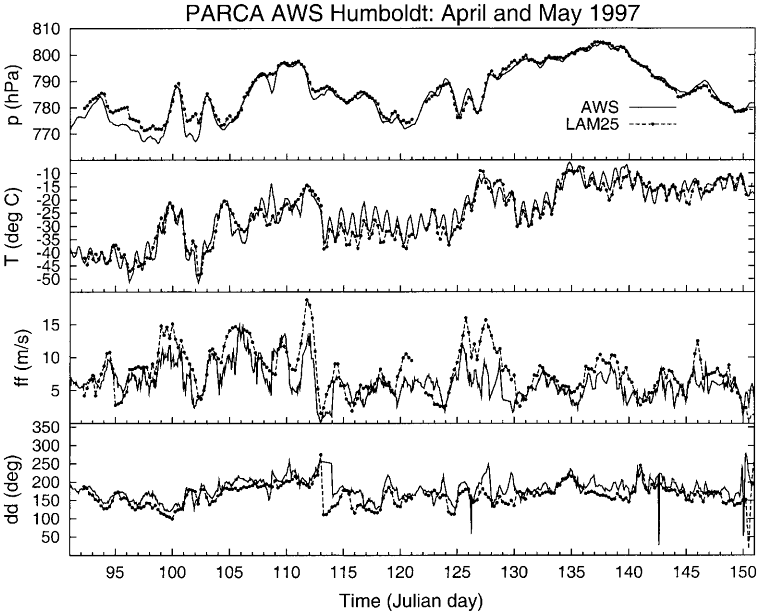

Fig. 3. Time series (April and May 1997) of NORLAM forecasts and observations of the surface pressure (p, first panel), near surface air temperature (T, second panel), wind speed (ff, third panel) and wind direction (dd, fourth panel) at PARCA AWS Humboldt (HU). AWS data (full lines) are given at the specific sensor heights, while for the NORLAM LAM25 results (dashed lines with filled circles) surface pressure at the elevation of the grid point, the 2 m temperature and the 10 m wind were used. No corrections for differences between the elevation of the model grid point and the reported elevation of the AWS were made. Julian days 91 and 121 correspond to 1 April 1997 and 1 May 1997, respectively. Model data lines start on the second day of each month at 0600 UTC, since only the +30 h, +36 h, +42 h and +48 h NORLAM output is used in the time series

resolution. Figure 4 displays a time series for KABEG AWS A4. Like at the location Humboldt, the modeled pressure and temperature agree well with the observations. The wind speed is also simulated relatively well, but again the NORLAM 10 m winds seem to overestimate episodes with stronger winds. The wind direction simulated by NORLAM also shows a good agreement with the measured wind direction.

In order to validate the model's ability to capture the main synoptic features, the station Summit (SU, in Fig. 1b) was chosen, since it is located on top of the Greenland ice sheet where the slope of the terrain is negligible. In contrast to the other AWS discussed in this paper, winds at Summit are not katabatically driven, but purely synoptically forced. It can be seen that the main synoptic features are captured well by NORLAM (Fig. 5). However, the simulated amplitudes of the daily courses of the near surface air temperature are too weak compared to the observed courses. Particularly during the second half of May 1997, when only very weak winds were present, the simulations of the temperature indicate the typical daily courses for almost cloudless conditions, but the temperatures are generally too low and the amplitudes too weak. This problem may be attributed to parameterization problems for strong stable stratification in the boundary layer. For other periods (e.g., the beginning of May) the model prediction of the cloud amount seems to be unrealistic, which leads to a complete suppression of the daily courses of the near surface air temperature. The excessive cloud amount in the model, which also prevents the development of the katabatic wind over the slopes (see Fig. 4, days 122–124), was found to result from high humidity values of the initial ECMWF analyses (see below). In contrast, the problem of the boundary layer parameterizations appears to be less important for the katabatic flow, where the stratification is less stable due to dynamical mixing.

In order to allow a better quantitative comparison, statistics of the variables surface pressure, near surface temperature, wind speed and wind direction are shown in Table 4 for five selected PARCA AWS for April and May 1997. For all five AWS, the correlation of the surface pressure of the

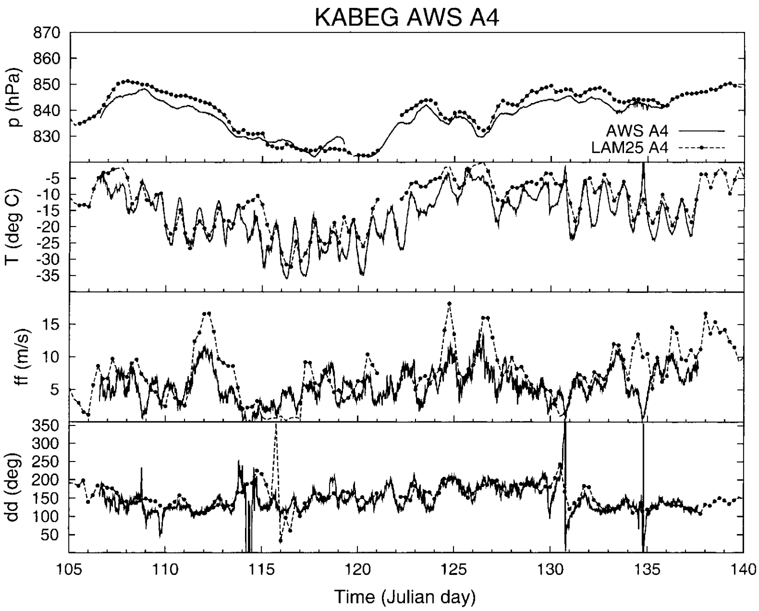

Fig. 4. Same as Fig. 3, but for KABEG AWS A4, and only for the time period of KABEG (about the second half of April 1997 and the first half of May 1997)

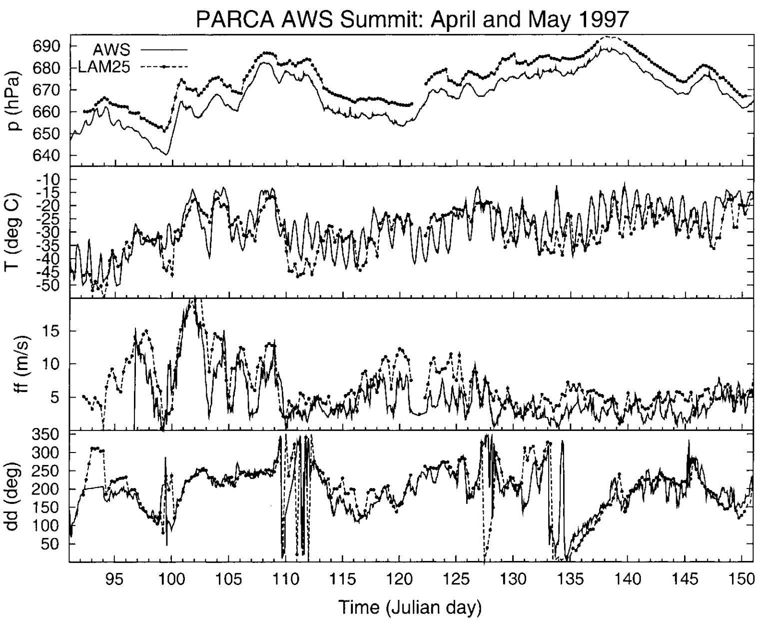

Fig. 5. Same as Fig. 3, but for AWS Summit (SU)

simulation results and the measurements is very good with values between 0.94 and 0.99. Some biases can be seen in pressure, which are partly due to the different heights of the model grid points and the AWS. The elevations of the AWS sites are known within the errors of the GPS measurements, which are ± 20 m for Summit and Crawford, and ± 0.1 m for Humboldt, Tunu and JAR1. However, the largest differences result from the averaging over the model grid size (25 km) and the fact that the model grid point closest to the AWS was taken, which represents a problem especially in the steeper coastal regions (JAR1). The model topography (using the TBASE 8 km resolution data set, see Table 2) has also lower elevations on top of the ice sheet, resulting in a relatively large pressure bias for Summit. The correlation coefficients of the 2 m temperature and the wind speed are relatively high apart from Summit in May 1997, where the mean wind speed is comparably low. Biases in temperature and wind speed are small for almost all AWS with absolute values of about 1–2 K and 1–2 ms^{-1}, respectively. Modeled wind speeds are generally slightly larger than measured speeds (apart from JAR1 in April 1997), which is partly due the

Table 4. Statistics of PARCA AWS and NORLAM simulations for selected AWS locations for April and May 1997. Mean (AWS), bias (NORLAM-AWS), standard deviation (stdv) and correlation coefficients between NORLAM and AWS (corr) of surface pressure, temperature and wind speed, respectively, and mean and bias of wind direction. Maximum absolute values are printed bold, minimum absolute values are underlined. AWS values are given at the individual sensor heights, while for the NORLAM the surface pressure at grid point height, the 2 m temperature and the 10 m wind were used. No corrections for differences between the elevation of the model grid point and the reported elevation of the AWS were made

station	month	surface pressure				temperature				wind speed				wind direction	
		mean (hPa)	bias (hPa)	stdv (hPa)	corr	mean (°C)	bias (°C)	stdv (°C)	corr	mean (ms^{-1})	bias (ms^{-1})	stdv (ms^{-1})	corr	mean (deg)	bias (deg)
Humboldt	April	780	2.18	2.10	0.97	−31.3	−0.97	3.75	0.90	7.1	1.65	2.29	0.78	179	**−18**
Humboldt	May	791	−0.19	1.31	**0.99**	−17.3	−0.70	2.76	0.91	5.5	1.54	2.48	0.61	183	**−18**
Tunu	April	777	1.21	**2.64**	0.94	−31.0	−1.97	3.82	0.88	6.3	**2.92**	2.61	0.80	277	16
Tunu	May	788	−0.24	2.12	0.96	−19.6	−2.52	2.98	0.88	5.4	2.45	1.69	0.68	277	17
Crawford	April	783	2.84	2.39	0.98	−22.7	0.90	4.79	0.87	6.0	2.12	2.83	0.69	148	−1
Crawford	May	795	1.07	1.53	0.98	−12.7	0.89	3.46	0.72	6.0	2.49	2.61	0.63	146	−8
JAR1	April	899	7.49	2.52	0.96	−15.5	0.81	3.01	0.94	5.8	−0.72	2.83	0.70	121	4
JAR1	May	906	5.96	1.67	0.97	−4.5	0.64	2.38	0.77	6.2	0.30	2.57	0.76	123	1
Summit	April	661	**7.89**	1.99	0.98	−31.1	−1.25	6.58	0.74	6.8	2.23	**2.88**	**0.81**	206	3
Summit	May	674	6.30	1.45	0.97	−23.9	**−2.60**	**6.69**	0.40	3.6	1.74	1.90	0.48	208	14

different heights (NORLAM 10 m/AWS about 2–4 m). The mean wind directions are simulated well by NORLAM with a maximum absolute bias of less than 20°.

3.2.2 A case study of the daily course of the katabatic wind system

The daily course of the katabatic wind during a selected time period (KABEG flights KA2/KA3, Table 5) will be described in more detail in this subsection, using the AWS measurements of KABEG station A4, which is located over the relatively homogeneous interior part of the ice sheet at a height of about 1600 m. The synoptic situation on 21 April 1997 (flight KA2) was characterized by a high pressure system over Central Greenland. Relatively strong pressure gradients were present north of the Kangerlussuaq area. The area, where the flight pattern was flown, was cloud-free, and strong winds and snow drift were observed during the flight.

On 22 April 1997 (flight KA3), the position of the strong high pressure system over Central Greenland was shifted southwards compared to the previous day. As a result of the southward movement of the high, the zone of the strongest pressure gradients was shifted as well. Therefore, relatively strong pressure gradients were present in the Kangerlussuaq area, which was completely cloud-free at that time. During the flight, very intense winds of more than 20 ms^{-1} and snow drift were observed.

In order to show the distribution of the near surface winds during a synoptically enforced katabatic wind case, the NORLAM-simulated winds at the lowest model level (roughly 10 m above ground) are displayed for the Kangerlussuaq area for 0600 UTC 22 April in Fig. 6. Strong katabatic winds with wind speeds of up to 18 ms^{-1} are present over the slopes. The complex structure of the tundra area is not resolved by the model, but its larger roughness length $(10^{-2}\,\mathrm{m})$ compared to the inland ice $(10^{-4}\,\mathrm{m})$ and the change in the topography gradient lead to a strong modification of the katabatic flow within about two grid points. The near surface wind field is very homogeneous in the area of the KABEG stations A1–A4.

In Fig. 7, measurements of A4 and model results at the nearest grid point to A4 are dis-

Table 5. List of the KABEG katabatic wind flights used for the comparison in April and May 1997, areas according to Fig. 2 (time in UTC)

Date, time	Flight	Area, profile	Time for the comparison aircraft/NORLAM
18 April 1997 0700–1145	KA1	K1, A4	0740/0800
21 April 1997 0630–1150	KA2	K1, A4	0710/0800
22 April 1997 0705–1210	KA3	K1, A4	0740/0800
29 April 1997 1020–1540	KA4	K1, A4	1100/1000
2 May 1997 0605–1150	KA5	K1, A4	0640/0600
11 May 1997 0635–1130	KA6	K2, P4	0810/0800
13 May 1997 0600–1205	KA8	K1, A4	0630/0600
14 May 1997 0600–1135	KA9	K3, I4	0710/0800

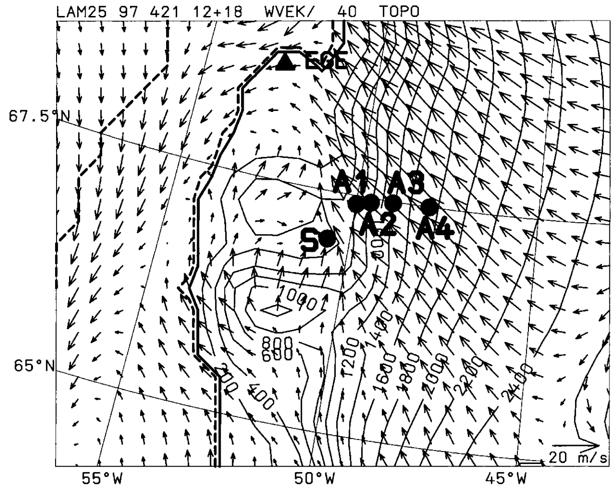

Fig. 6. Topography (isolines every 200 m) and wind vectors at the lowest NORLAM σ-level (about 10 m above ground) for KABEG flight KA3 valid at 0600 UTC 22 April 1997 obtained by an 18 h LAM25 simulation. The thick full line marks the coastline, while the thick dashed line indicates the position of the sea ice edge. The Greenland radiosonde station Egedesminde is indicated by a triangle; filled circles show the positions of the KABEG AWS (A1 in the tundra, A2–A4 over the ice, S near Kangerlussuaq)

played for the period of 21 April to 23 April. A4 was designed as an energy balance station, and profiles of wind speed and air temperature (3 levels) as well as snow temperatures (5 levels) and net radiation were measured. Turbulent fluxes of momentum and sensible heat (H) were calculated using a variational approach similar to Xu and Qiu (1997). With the decrease of the net radiation during nighttime (from 21 to 22 April), a significant cooling of the surface layer begins, which is slightly underestimated by the numerical model. Additionally, the simulated cooling seems to occur slower than the observed cooling, i.e. a phase difference is present. Parallel to the decrease in temperature, an increase in wind speed can be seen. Although the model strongly overestimates the magnitude of the wind speed, the qualitative development in time is captured well. After sunrise, the net radiation increases again, and the warming of the surface layer is obvious. With this warming during daytime, the intensity of the katabatic winds reduces, and a turning of the winds to a more contour-parallel flow can be seen from the observation. This change in wind direction during daytime is underestimated by NORLAM by about 20°.

The shown daily course of the near surface wind at A4 for the period of 21 April to 23 April is strongly influenced by the presence of a pronounced synoptic pressure gradient (not shown). This results in an increase of the wind speed even during the period of positive net radiation on 21 April. For the night of 21 to 22 April, the wind field is influenced by the synoptic forcing and the katabatic forcing. Heinemann (1999) shows for cases with weak synoptic forcing that a pronounced daily cycle of the near-surface wind is present over the ice due to the nighttime development of the katabatic wind with a peak to peak amplitude of 5 ms^{-1} for the wind speed anomaly. The onset of the katabatic wind is found to occur at about two hours before sunset, and the wind speed maximum is observed in the early morning hours. However, a pronounced diurnal cycle is present for all katabatic wind days (weak and strong synoptic forcing) for the net radiation, wind direction and temperature.

The model simulations can also be compared with measured components of the surface energy balance. A good agreement is found for the net radiation (Q) and the sensible heat flux (H). During nighttime and high wind speeds, the energy loss

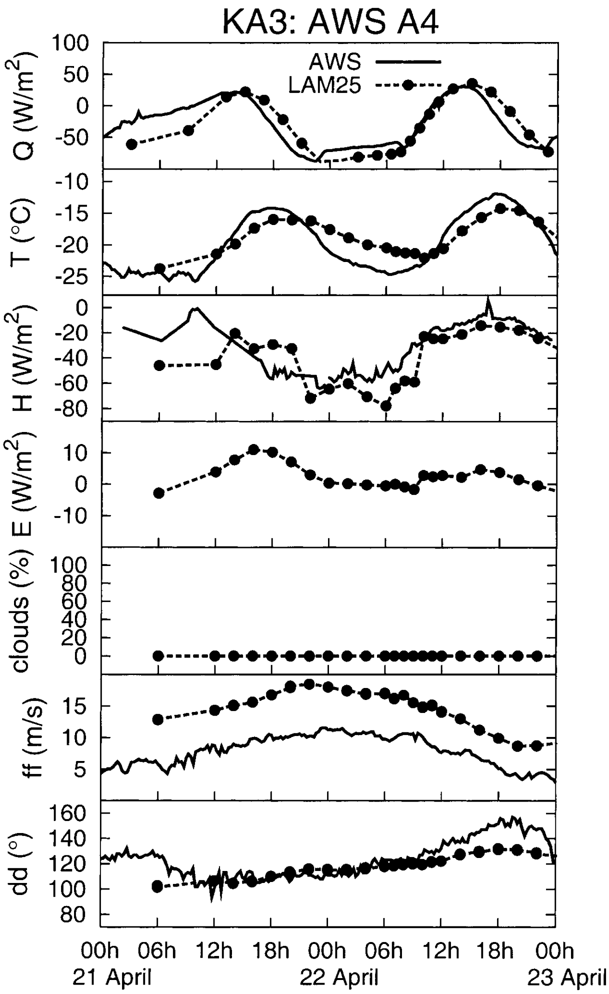

Fig. 7. Two day time series of NORLAM results and observations at KABEG AWS A4 for the period of 21 April to 23 April 1997. The displayed variables are (from top to bottom): Net radiation (Q), 2 m temperature (T), surface fluxes of sensible (H) and latent (E) heat, total cloud coverage, wind speed (ff) and direction (dd) at 10 m (LAM25) and sensor height (AWS), respectively. LAM25 results are dashed with filled circles, AWS values are plotted with full lines

by the net radiation is almost completely compensated by a flux of sensible heat towards the surface. Modeled evaporation (E) is very small as could be expected for the air temperatures being in the range of −15 °C to −25 °C.

3.3 Comparisons of aircraft data and simulated boundary layer profiles

NORLAM's ability to correctly simulate the vertical structure of the katabatic wind system and its development in time was investigated by comparisons of aircraft-measured and simulated vertical profiles for all KABEG cases except KA7 on 11 May 1997, which was flown after KA6, when the katabatic wind system had already decayed (Table 5). A selection of KABEG cases with highly different synoptic conditions is discussed more elaborately in this section. As locations for the comparisons, the highest reference points of the individual flight tracks were chosen, since they were located over relatively homogeneous terrain and farthest from the ice edge. Figure 2 shows the typical flight pattern for the Kangerlussuaq region (area K1) and the flight patterns for the Angmagssalik flight program (area K2) and the Ilulissat flight (area K3, see Table 5). For the Kangerlussuaq region, the highest position along the flight track (Pb in Fig. 2) is relatively close to the location of KABEG AWS A4 (67.498° N, 47.997° W), which was chosen for the comparisons. For the comparison to model data, the aircraft temps were horizontally averaged with a radius of about 25 km, while an averaging radius of 10 m was used vertically. The averaged boundary layer profiles are slightly smoother than individual profiles, and are more appropriate for intercomparisons with model data. For the Angmagssalik and Ilulissat flights, the locations P4/Pa (65.947° N, 41.153° W in the K2 area) and I4/Pd (69.367° N, 48.000° W in the K3 area) were chosen for the profile comparisons.

3.3.1 KA1

KABEG flight KA1 took place on 18 April 1997. At that time, a high pressure system over South-eastern Greenland provided a weak southerly synoptic flow in the area of Kangerlussuaq. Some stratus clouds were present over the tundra area, while the ice sheet was cloud-free.

Figure 8 shows vertical profiles of wind speed, potential temperature and wind direction for 18 April 1997 at 0600 UTC/0800 UTC (NORLAM, 30 h and 32 h prognoses) and about 0740 UTC (observation, aircraft and A4 data). The two modeled profiles as well as the aircraft obtained profile show the typical vertical structure of the katabatic wind system. While the 'nose' of the observed wind speed profile (low-level jet, LLJ) is located at a height of about 80 m, the model simulates the LLJ at a height of about 50 m. The model underestimates the intensity of the kata-

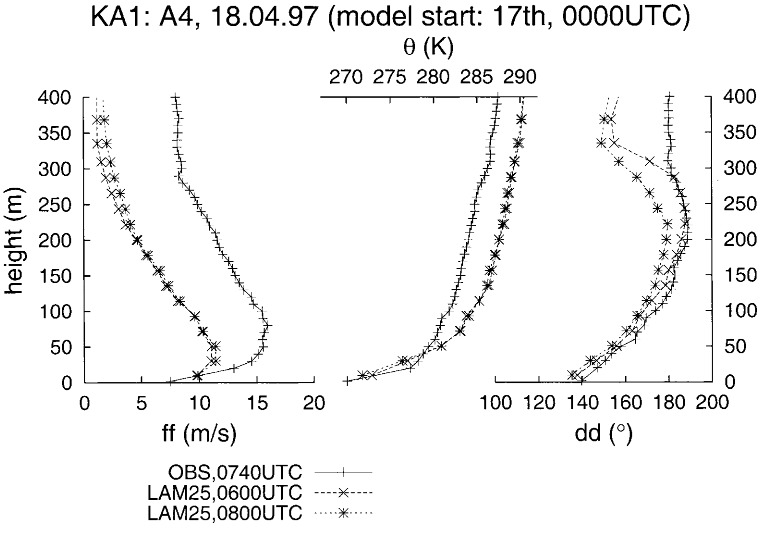

Fig. 8. Observed (OBS, aircraft and A4) and simulated profiles using the 30 h and 32 h forecast of the LAM25 (started at 0000 UTC 17 April) at location A4 during KA1. The displayed variables are wind speed (ff), potential temperature (θ) and wind direction (dd)

batic winds by about 5 ms^{-1} and above 300 m by an even larger value. At 400 m, the aircraft observations still show wind speeds of about 10 ms^{-1}. The large differences at upper levels (300–400 m) suggest that some upper level synoptic support of the katabatic winds is missing in the NORLAM forecast. Comparisons of the ECMWF analysis for 0000 UTC 18 April to the NORLAM forecasts of the model runs started 24 h/12 h before show slight differences in the location of a strong pressure gradient zone. This could either be due to a wrong prognosis of the NORLAM or to an insufficient quality of the ECMWF analysis for 17 April used as initial fields for the NORLAM runs.

The vertical structure of the potential temperature shows the typical strong inversion pattern for katabatic wind cases in the modeled profiles. The observed surface inversion was too thin to be resolved by the aircraft measurements, but is indicated by the low 2 m temperature of the KABEG AWS A4. The vertical profile of the wind direction is reproduced very well by the model. Differences only occur at heights above 200–300 m, where only weak winds are present in the model. A significant turning of the wind can be seen from a near surface direction of about 140° to a more cross-slope direction of about 190° at a height of 200 m.

The forecast using the analysis of 1200 UTC 17 April as initial field did not lead to a significant improvement, but the model run started at 0000 UTC 18 April shows a much better agreement in the wind speed profile at heights above 250 m (Fig. 9). Yet, the lower structure of the profile is still not captured very well by the model, which can be attributed to the relatively short spinup time of the model in this simulation. The results of the KA1 simulations using different start times reveal a general problem of the numerical simulation of katabatic wind cases. On the one hand, the model should be started with an analysis close to the time of the flight in order to capture the synoptic conditions best, while on the other hand the model has to be given a sufficient spinup time to build up a realistic boundary layer structure.

3.3.2 KA3

As described in Sect. 3.2, KA3 was one of the cases when a relatively strong synoptic pressure gradient was present in the Kangerlussuaq area. Figure 10 shows the vertical profiles measured on 22 April 1997 at about 0740 UTC and profiles valid at 0600 UTC, 0800 UTC and 1000 UTC of a NORLAM simulation started at 0000 UTC 21 April. The simulated profile at 0800 UTC for this case almost exactly captures the observed structure and magnitude of the wind speed profile in the lowest 120 m of the boundary layer (particularly the height of the LLJ). Above that height, the agreement is still good, although differences of about 1–2 ms^{-1} in wind speed occur at heights between 120 m and 350 m. The model profile valid at 1000 UTC agrees almost exactly with the observed profile at heights above 150 m, while the simulated wind speeds below that level are weaker than the observations at 0740 UTC. This reflects the diurnal development of the katabatic wind

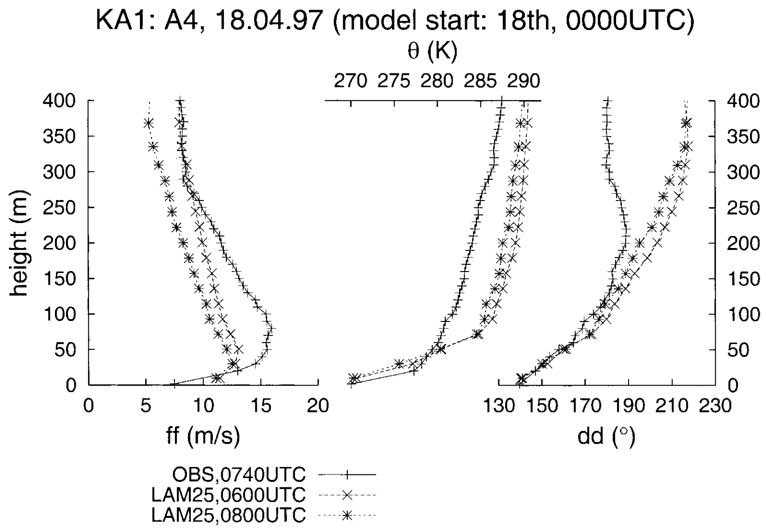

Fig. 9. Same as Fig. 8, but for the 06 h and 08 h forecast of a LAM25 run started at 0000 UTC 18 April

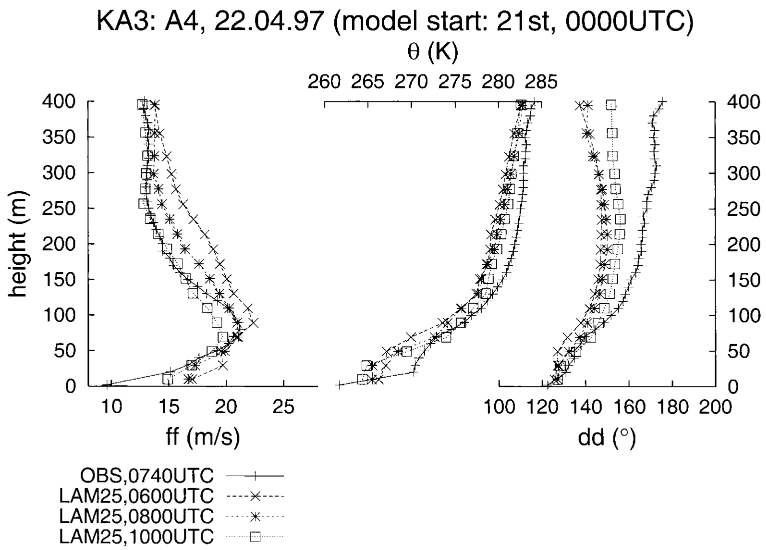

Fig. 10. Same as Fig. 8, but for KA3 and simulated profiles from the 30 h, 32 h and 34 h forecast of the LAM25 (started at 0000 UTC 21 April)

system, which decays significantly during the daytime due to the reduction of the katabatic and synoptic forcing. This effect is even more pronounced in the model profile at 1200 UTC (not depicted), where the wind speeds are about 3–5 ms^{-1} less than at 0600 UTC. This modeled decay of the katabatic wind system is in agreement with the aircraft temps flown later on the same day (at about 1000 UTC, not displayed).

As expected considering the very good agreement of the modeled wind speeds with the observations, the potential temperature profile is also captured very well by the model. Like in the case KA1 discussed above, slightly larger differences only occur close to the surface in the lowest 50–100 m (differences of up to 5 K). The main differences are the height of the stable boundary layer (SBL) and the temperature in the lowest 50 m. The flat layer of about 30 m vertical extent above ground with a nearly neutral stratification agrees with the observations, which are 3–4 K warmer than the simulations in this lower part of the boundary layer, but the 2 m temperature of the AWS indicates that the very shallow inversion in the surface layer is not captured by the simulations.

The wind direction is simulated very well in the lowest 100–150 m and changes only slightly in time. At higher levels, the differences between simulations and observations increase to about 30° considering the model profiles at 0600 UTC and at 0800 UTC, while the profile at 1000 UTC only shows differences up to 20°. The model profile at 1200 UTC (not displayed) nearly exactly reproduces the observed wind direction profile. The better agreement in wind direction at upper levels for the later profiles at 1000 UTC and 1200 UTC indicates that the model also simulates the right synoptic conditions for that case, but obviously with a small time difference of about 2–4 h.

The LAM25 simulation started at 1200 UTC 21 April (not shown) also yields a very good agreement in wind speed and potential temperature while capturing the wind direction almost exactly. In a simulation started 12 h later (at 0000 UTC 22 April, not shown), the model still captures the observed vertical structure of the wind direction and the potential temperature very well, but the LLJ is less pronounced and wind speeds at heights between 150 m and 350 m are overestimated by up to 5 ms^{-1}. This indicates that the spinup time of only 6 hours for the latter simulation is probably not sufficient for the case of the strong katabatic wind system during KA3.

3.3.3 KA9

For the katabatic wind flight KA9 (14 May 1997, see Table 5) the region of Ilulissat Glacier was chosen, which is located north of the Kangerlussuaq area (compare area K1 and K3 in Fig. 2). The synoptic situation is characterized by a high pressure system over Central Greenland. A cloud coverage of about 3/8 Ci was present over the inland ice, and in some areas even low clouds (1/8 Sc) were observed.

The aircraft measurements show a pronounced wind maximum of 15 ms^{-1} at a height of about 70 m for that case (Fig. 11). The LLJ is almost exactly simulated by the NORLAM forecast started at 1200 UTC 13 May 1997. Only slight differences in wind speed of 1–3 ms^{-1} are present at heights between 150 m and 350 m. Potential temperature and wind direction of observation and model are also in very good agreement. Larger differences in wind direction are noticeable at heights above about 300 m, where the simulated and observed wind speed are relatively small. In the case of KA9, the NORLAM forecast started at 1200 UTC 13 May 1997 (Fig. 11) yields the best agreement with the observation. The simulation started 12 h earlier overestimates the wind speeds at upper levels, while for the model run started 12 h later (14 May 1997 at 0000 UTC) the spinup time of the model appears to be too short, which leads to an underestimation of the observed wind speeds.

3.3.4 Profile statistics

After the elaborate discussion of selected KABEG flights above, a more compact analysis of the quality of the NORLAM simulations is added in this subsection. Several statistics of the investigated profiles are presented in Table 6. For most simulations, the biases (NORLAM minus observation) in wind speed are relatively small with values of about 1–3 ms^{-1}. However, for those cases, where the synoptic conditions are not well captured (i.e., for the longer forecasts for KA1,

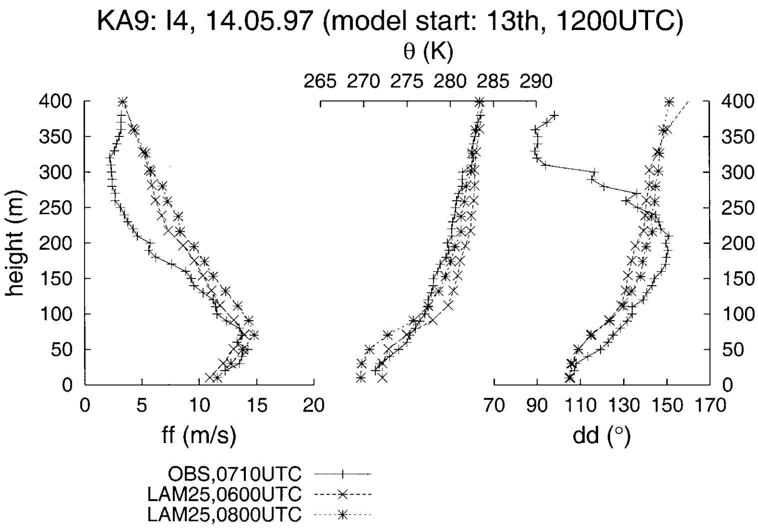

Fig. 11. Same as Fig. 8, but for KA9 and simulated profiles from the 18 h and 20 h forecast of the LAM25 (started at 1200 UTC 13 May) at location I4 (Ilulissat region)

Table 6. Statistics from the comparison of the NORLAM-simulated vertical profiles of the runs with different model start times to the aircraft-observed vertical profiles during the KABEG flights (see Table 5 for comparison times). The letters "nc" after a flight name indicate a "no cloud run" (artificially suppressed cloud development). Bias is the mean difference NORLAM minus observations, and "stdv" and "corr" are the standard deviation and the correlation coefficient between NORLAM and aircraft data, respectively. Maximum absolute values are printed bold, minimum absolute values are underlined. "Long", "medium" and "short" refer to averages for the different NORLAM forecast times (taking the "no cloud run" for KA4 and KA5)

Flight number, forecast time	Potential temperature									Wind speed								
	bias °C			stdv °C			corr %			bias ms^{-1}			stdv ms^{-1}			corr %		
KA1, +32/+20/+08	2.9	2.3	3.1	1.2	1.7	1.5	97	92	92	−6.0	−4.9	−3.2	1.1	1.4	1.0	95	89	95
KA2, +32/+20/+08	1.6	1.0	1.8	1.9	1.5	1.7	89	99	85	−5.7	−4.9	2.6	2.8	2.5	0.7	44	79	98
KA3, +32/+20/+08	−1.8	−0.7	0.4	1.0	1.7	1.6	**98**	93	94	1.0	−1.9	−0.2	0.6	1.1	1.5	98	92	86
KA4, +34/+22/+10	2.2	2.5	2.8	1.7	2.3	1.4	88	91	97	−1.5	−0.6	0.7	1.3	2.2	1.1	48	−92	78
KA4nc, +34/+22/+10	0.8	0.7	2.0	1.5	1.2	1.3	89	92	86	1.6	2.0	1.3	0.7	0.6	0.6	92	93	92
KA5, +30/+18/+06	**3.4**	2.7	2.8	**3.2**	2.8	2.0	97	92	93	0.0	0.6	2.3	**3.4**	2.7	2.0	−69	63	92
KA5nc, +30/+18/+06	1.2	1.2	2.9	1.3	1.4	2.0	94	93	88	0.8	0.6	2.1	1.6	1.4	2.1	90	93	92
KA6, +32/+20/+08	−0.1	0.4	2.3	1.5	1.0	0.9	93	97	97	−9.1	−7.0	−2.4	1.0	0.9	0.3	83	**99**	**99**
KA8, +32/+20/+08	−0.8	−1.1	1.6	1.2	1.4	1.9	**98**	97	95	−6.8	**−10.0**	−6.8	2.6	2.9	2.4	65	64	70
KA9, +32/+20/+08	1.8	0.1	4.5	1.8	1.3	0.7	95	97	**98**	8.0	2.4	−2.0	3.1	1.5	1.3	85	96	98
Average long/medium/short	0.7	0.5	2.3	1.4	1.4	1.5	94	95	92	−2.0	−3.0	−1.0	1.7	1.5	1.2	82	88	91

KA2, KA6 and KA9, and for KA8), the biases are larger with values of up to 10 ms^{-1}. In the cases KA4 and KA5, NORLAM erroneously predicted clouds, preventing the development of the katabatic wind system. A neutral stratification and no LLJ is simulated for KA4, which results in a negative correlation for the wind speed profile for the +22 h forecast. 'No cloud runs' (sensitivity studies with artificially suppressed cloud development in the model) for KA4 and KA5 lead to a much better simulation of the wind speed while slightly reducing the correlation of the potential temperature as a result of an overestimation of the inversion strength. This result shows that a realistic simulation of clouds is a crucial requirement for the success of katabatic wind simulations. If the model overestimates the cloud coverage (particularly low clouds), the katabatic wind development is too weak compared to the observations. Potential reasons for wrong cloud forecasts can be wrong moisture fields in the forcing model, wrong NORLAM forecasts, or a general problem with the cloud physics scheme of the model like an overestimation of the cloud thicknesses or the clouds' optical thicknesses. Since the NORLAM cloud cover is determined diagnostically based on the relative humidity and the vertical velocity, its cloud prediction could be directly affected by a potential moisture excess in the ECMWF analyses. This is the case particularly for KA4, when the ECMWF analyses used as initial fields showed values for the relative humidity exceeding 80% in the lowest 1000 m over the ice surface in the Kangerlussuaq area.

In order to provide a more compact measure of the quality of the simulations, average values of the statistical parameters are shown in Table 6 for all katabatic wind simulations apart from the standard runs for KA4 and KA5, where the results of the respective "no cloud run" were taken instead. The simulations started about 30–34 h prior to the flights are referred to as "long range forecasts" ("long" in Table 6). The simulations started about 18–22 h prior to the observations are called "medium range forecasts" ("medium" in Table 6), and the model runs started closest to the time of the flights (about 6–10 h prior) are named "short range forecasts" ("short" in Table 6). The average bias and standard deviation in wind speed is smallest for the short range forecast of the katabatic wind profiles. The standard deviations are generally relatively small with an average value of about 1.5 ms^{-1}. Correlation coefficients show a very good correlation with best average values for the short range forecast. The biases and standard deviations of the potential temperature profiles however are smallest for the medium range forecast, and the correlations are largest.

The different forecast qualities dependent on the forecast time demonstrate that the spinup time is a key issue for the simulation of the strong katabatic wind system. A longer spin-up time results in a better simulation of the inversion structure, while the simulation of the synoptic forcing on the wind profile gets worse with increasing forecast time. Forecast times of 18–22 hours seem to be a good compromise between sufficient spin-up time and the forecast of the synoptic forcing on the katabatic wind system.

4. Summary and conclusions

Numerical simulations with the mesoscale model NORLAM have been performed for two complete spring months (April and May 1997) and for individual cases covered by aircraft investigations of the KABEG experiment. The comparisons of the NORLAM forecasts to AWS data of KABEG and the PARCA GC-Net and to aircraft observations of KABEG yield an overall very satisfying agreement of model and observations.

From the simulations, some essential requirements are necessary for a successful forecast of the boundary layer and katabatic winds over the Greenland ice sheet using mesoscale limited models. The success of the simulation of katabatic winds over the Greenland ice sheet is crucially depending on the correct forecast of the synoptic conditions, since the structure and intensity of the katabatic wind system strongly depends on the synoptic environment. It is therefore of great importance that the initial data for the simulations capture the synoptic pressure fields well. Additionally, good moisture analyses are necessary as initial fields for the mesoscale model. If the analyses are too moist, an overestimation of clouds by the mesoscale model is likely. A wrong cloud prediction consequently leads to a wrong prediction of the boundary-layer development, i.e. the nighttime cooling due to the divergence of the net radiation, which is one essential driving mechanism of katabatic winds.

Besides these requirements concerning the initial data, the mesoscale model itself has to realistically predict the synoptic environment and the SBL development in order to yield a correct katabatic wind forecast. The incorrect simulation of clouds in two of the examined cases clearly indicate the need for advanced cloud prediction schemes for katabatic wind forecasting on an operational basis. Another requirement is a sufficient vertical resolution of the SBL in the model, which was 18 model layers in the lowest 400 m in our simulations.

The comparison of the NORLAM simulations to the KABEG aircraft data and AWS measurements shows encouraging results and confirms that the basic physics of katabatic winds are well captured by the model. The good quantitative agreement of the simulations with the observational data indicates that – taking into account the above-mentioned requirements – the katabatic wind system is simulated well even with a low-order boundary layer parameterization such as Louis (1979). Yet, the complex four-dimensional structure of katabatic winds close to the coast and in the vicinity of the transition region between ice sheet and tundra near the Kangerlussuaq region can not be simulated by a mesoscale model with 25 km grid spacing. This effort would require resolutions of less than 5 km in order to provide a satisfactory description of the small-scale topography of the Greenland coastal areas and has to be left for future work.

Since the katabatic wind system over Greenland and Antarctica is of major importance in many research fields like for instance glaciology, and since it has a crucial impact on human life and activities in polar regions in the vicinity of the slopes of the ice sheet, it is essential to broaden the scientific understanding of this atmospheric phenomenon and to significantly improve weather prediction models applied for katabatic wind forecasting and katabatic wind simulations. The present study is a first step to validate a mesoscale numerical model using four-dimensional observational data of katabatic winds in a remote area, where validation data sets are generally quite rare.

Acknowledgements

The present study was funded by the Deutsche Forschungsgemeinschaft (DFG) under grant He 2740/1 and by the ACSYS project of the Bundesministerium für Bildung und Forschung under Grant No. 03PLO20F. KABEG was an experiment of the Meteorologisches Institut der Universität Bonn (MIUB) in cooperation with the Alfred-Wegener-Institut (AWI). The Deutscher Akademischer Austauschdienst (DAAD) and the National Science Foundation (NSF) provided the travel funding (grant 315/ppp) for the cooperation between the MIUB and the Byrd Polar Research Center at the Ohio State University. The ECMWF provided the analyses taken as initial and boundary conditions for the simulations. The Norwegian Meteorological Institute (DNMI) at Oslo made the NORLAM model available. SSM/I data used for the derivation of the sea ice coverage for April and May 1997 were provided by the Global Hydrology Resource Center (GHRC) at the Global Hydrology and Climate Center (Huntsville, Alabama, USA). Thanks go to Konrad Steffen and Jason Box of the University of Colorado at Boulder, who made the AWS data of the Greenland Climate Network available. The authors are grateful to Clemens Drüe and Ulrike Falk of the MIUB, who contributed to a successful setup of the KABEG stations and data evaluation.

References

Ball FK (1956) The theory of strong katabatic winds. Aust J Phys 9: 373–386

Ball FK (1960) Winds on the ice slopes of Antarctica. Antarctic Meteorology. Proc Symposium, Pergamon Press, pp 9–16

Blackadar AK (1979) High resolution models of the planetary boundary layer. Advances in Environment and Scientific Engineering. London: Gordon and Breach, 276 pp

Bratseth A (1982) A simple and efficient approach to the initialization of weather prediction models. Tellus 34: 352–357

Bromwich DH, Du Y, Parish TR (1994) Numerical simulation of winter katabatic winds from West Antarctica crossing Siple Coast and the Ross Ice Shelf. Mon Wea Rev 122: 1417–1435

Bromwich DH, Du Y, Hines KM (1996) Wintertime surface winds over the Greenland ice sheet. Mon Wea Rev 124: 1941–1947

Cavalieri DJ, St. Germain KM, Swift CT (1995) Reduction of weather effects in the calculation of sea-ice concentration with the DMSP SSM/I. J Glaciol 41: 455–464

Ekholm S (1996) A full coverage, high-resolution, topographic model of Greenland computed from a variety of digital elevation data. J Geophys Res 101: 21961–21972

Forrer J, Rotach MW (1997) On the structure in the stable boundary layer over the Greenland ice sheet. Boundary Layer Meteorol 85: 111–136

Gallée H (1995) Mesoscale atmospheric circulations over the southwestern Ross sea sector, Antarctica. J Appl Meteor 35: 1129–1141

Grønås S, Hellevik OE (1982) A limited area prediction model at the Norwegian Meteorological Institute. Technical Report No. 61, The Norwegian Meteorological Institute, Oslo, Norway

Heinemann G (1996) Katabatic wind systems over polar ice sheets. Proc 6th Workshop on Mass Balance of the Greenland Ice Sheet and Related Topics, 22–23 January 1996, Copenhagen, Denmark. Published by the Geological Survey of Greenland, Copenhagen, Report No. 53, pp 39–43

Heinemann G (1997) Idealized simulations of the Antarctic katabatic wind system with a three-dimensional mesoscale model. J Geophys Res 102: 13825–13834

Heinemann G (1998) Katabatic wind and Boundary Layer Front Experiment around Greenland (“KABEG’97”). Reports on Polar Research 269. Alfred Wegener-Institut für Polar- und Meeresforschung, 93 pp

Heinemann G (1999) The KABEG’97 field experiment: An aircraft-based study of katabatic wind dynamics over the Greenland ice sheet. Boundary Layer Meteorol 93: 75–116

Hines KM, Bromwich DH, Parish TR (1995) A mesoscale modeling study of the atmospheric circulation of high southern latitudes. Mon Wea Rev 123: 1146–1165

Kuo HL (1965) On formation and intensification of tropical cyclones through latent heat release by cumulus convection. J Atmos Sci 22: 40–63

Louis J-F (1979) A parametric model of vertical eddy fluxes in the atmosphere. Boundary Layer Meteorol 17: 187–202

Meesters A, Bink N, Henneken E, Vugts H, Cannemeijer F (1997) Katabatic wind profiles over the Greenland ice sheet: observation and modelling. Boundary Layer Meteorol 85: 475–496

NOAA (1995) TerrainBase Global DTM Version 1.0. NESDIS National Geophysical Data Center, Boulder Colorado 80303–3328, U.S.A

Nordeng TE (1986) Parameterization of Physical Processes in a Three-Dimensional Numerical Weather Prediction Model. Technical Report No. 65, The Norwegian Meteorological Institute, Oslo, Norway

Oerlemans J, Vugts HF (1993) A meteorological experiment in the melting zone of the Greenland ice sheet. Bull Amer Meteor Soc 74: 355–365

Parish TR, Bromwich DH (1987) The surface wind field over the Antarctic ice sheets. Nature 328: 51–54

Putnins P (1970) The climate of Greenland. In: Climates of the polar regions (Orvig S, ed.), World Survey of Climatology 14: 3–113

Rasmussen L (1989) Greenland winds and satellite imagery. Vejret, Danish Meteorological Society, pp 32–37

Reynolds RW, Smith TM (1994) Improved global sea surface temperature analyses using optimum interpolation. J Climate 7: 929–948

Steffen K, Box JE, Abdalati W (1996) Greenland Climate Network: GC-Net. Special Report on Glaciers, Ice Sheets and Volcanoes, Tribute to M Meier, SC Colbeck (eds), CRREL Special Report 96–27, pp 98–103

Wendler G (1990) Strong gravity flow observed along the slope of eastern Antarctica. Meteorol Atmos Phys 43: 127–135

Xu Q, Qiu C-J (1997) A variational method for computing surface heat fluxes from ARM surface energy and radiation balance systems. J Appl Meteor 36: 3–11

Authors’ addresses: Günther Heinemann and Thomas Klein, Meteorologisches Institut der Universität Bonn, Auf dem Hügel 20, D-53121 Bonn, Germany, (E-mail: gheinemann@uni-bonn.de); David H. Bromwich, John J. Cassano, and Keith M. Hines, Polar Meteorology Group, Byrd Polar Research Center, The Ohio State University, USA; David H. Bromwich, Atmospheric Science Program, Department of Geography, The Ohio State University, USA